

SPACE EVENT DETECTION VIA ROBUST TIME SERIES FORECASTING

Pradipto Ghosh*

The ability to detect sudden and unexpected changes in the ephemerides of tracked space objects is a crucial feature of space event monitoring systems. These changes may arise from actual space events such as satellite maneuvers or collisions, from cross-tagging of space objects as might occur during a fly-by, or even from inadvertently introduced defects in the orbit determination (OD) workflow. Utilizing robust time series forecasting techniques, this paper introduces a new method for detecting sudden changes in the ephemeris of a tracked object. Test cases drawn from known space events demonstrate that the software implementation of this method is able to flag each sequentially supplied orbit-determined state as in- or out-of-family depending on whether the state is statistically typical relative to a configurable look-back interval.

INTRODUCTION

The principal goal of Space Situational Awareness (SSA) is “understanding and maintaining awareness of the Earth orbital population, the space environment, and possible threats.”¹ Implicit in this somewhat broadly stated objective is the need to be able to detect, or be aware of the involvement of a tracked Resident Space Object (RSO) in any situation that has caused it to behave in a manner that is atypical relative to its historically known behavior. The RSO in question may be a space asset whose operational well-being is of paramount importance from an economic or national security standpoint, thus making it crucial to be able to capture anomalies in its trajectory, or the object could be a satellite suspected of possessing malicious intent whose out-of-character trajectory changes must be noted prior to initiating further investigation. This paper presents a new method for detecting space events given observed historical and current orbit state data by utilizing a univariate time series forecasting method that is insensitive to the presence of past-event-generated outliers in the data.

In one of the earliest works published in the open literature on systematically detecting space events based on an existing database of tracked RSOs, Patera proposed a moving-window polynomial filtering method to detect aberrant behavior in orbit elements.² The basic idea there is to perform piecewise polynomial curve fit (in the least square sense) over sets of historical trajectory data, compute the standard deviation of the fit error between actual data and the fitted surface at pre-determined points, and then ascertain whether each error value exceeds the computed standard deviation by a user-specified ratio. Although the polynomial degree and least square fit span are “tunable” parameters in Patera’s work, no guideline is provided as to their choice. Swartz Jr. et al. adopted Patera’s work to create a web-based space event monitoring system, and extended it by

* Astrodynamics Engineer, Analytical Graphics Inc., 220 Valley Creek Blvd., Exton, Pennsylvania 19341-2380, U.S.A.
E-mail: pghosh@agi.com. Member AIAA.

presenting a systematic method of selecting the tunable parameters.³ Algorithms of both references 2 and 3 utilize Two Line Elements (TLEs) of tracked space objects as historic ephemeris information. Yet another method of capturing anomalous elements in orbit data sequence was put forward by Kelecy et al. which specifically focused on maneuver detection.⁴ This method also used TLE history to “learn” the to-date behavior of the orbit elements as a function of time, and is qualitatively similar to the Patera method in that it also involved filtering the data by a polynomial fit. Maneuvers are detected by comparing the difference between adjacent filtered segments with a user specified threshold factor of the fit-error standard deviation. More recently, using TLE history as an input, Lemmens and Krag reported a robust statistics-based maneuver detection method targeted particularly for LEO satellites.⁵ The present research also applies robust statistical time series analysis methods for identifying out-of-family OD data, but differs from the Lemmens and Krag work in two significant aspects:

- i) Lemmens and Krag pre-process an orbit element sequence by removing bias and certain harmonic components before handing over control to a core maneuver detection module that consists of fitting Thiel-Sen regression lines to local data windows and inter-quartile range computation as outlier threshold determiner. The method presented herein, on the other hand, applies exponential and Holt forecasting methods on an orbit element time series to predict an expected numerical value of the element. It is in weeding out outliers in the input TLE-derived time series that robust statistical methods are utilized.
- ii) Whereas the Lemmens and Krag procedure is geared specifically toward LEO RSO maneuver detection, the focus of this paper is on detecting abrupt changes in one or more orbital parameters that may be indicative of a space event. Such an event is loosely referred to as “maneuver” in this paper provided that the observed element value is different from the predicted value by large margin; otherwise an anomaly is simply noted. Having detected an anomalous element, an in-plane or out-of-plane maneuver may be *suggested* as *likely* if the discrepancy is large enough, but no claim is made regarding the correct label of the event causing it; rather, the intent is to raise an alert for undertaking further investigations.

The following section elucidates the space event detection algorithm, including the basic mathematical machinery and its software implementation. Test cases are presented next to demonstrate the utility of the presented method in identifying orbit data anomaly, and finally, conclusions are drawn.

SPACE EVENT DETECTION ALGORITHM

The basic concept underlying the validation of newly-received OD data as adopted in this paper is simple: as soon as a new orbit state becomes available, one or more of its components is compared with the corresponding forecast value based on its to-date sequence. If the forecast error is extraordinarily high, an anomaly is suggested. This value, or a more “typical” value if it is deemed an outlier, is then added to the data set to produce a new time series that is utilized for prediction and comparison for the next orbit state data, and this process is repeated. Fig. 1 schematically depicts the concept. Prediction is performed using robust *exponential* and *Holt smoothers*, the classical versions of which have traditionally found wide use in short-term financial time series forecasting.⁶ By default, the exponential smoothing model is used on an element sequence, unless it is expected to demonstrate a trend, in which case Holt’s model is used. Examples of trended orbit elements are the

semi-major axis of an uncontrolled LEO RSO subject to natural, drag-induced decay, or the mean RAAN and argument of perigee under the secular perturbative effect of the second zonal harmonic (J_2).

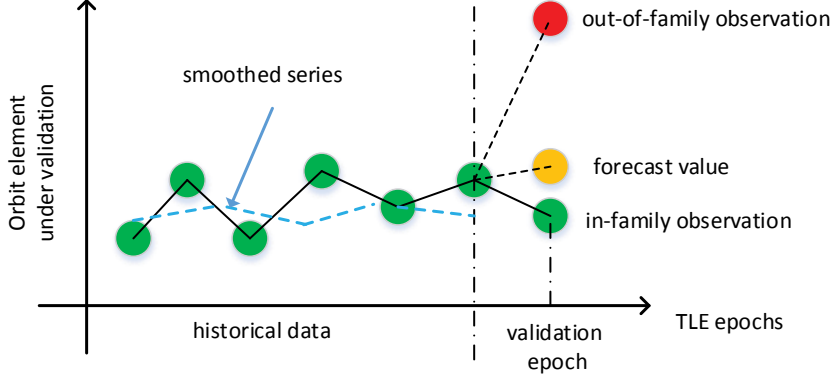


Figure 1: Outlier detection using time series forecasting

Mathematical Framework

Let $\mathbf{x}_t = [a_t \ e_t \ i_t \ \omega_t \ \Omega_t]^T$ be the OD state under examination, and $\xi = \{\xi_k : k \in \mathbb{I}\}$ be a given evenly-spaced scalar time series of an orbit element with $\mathbb{I} = \{1, 2, \dots, t\}$ being the index set and $\xi_k \in \{a_k, e_k, i_k, \omega_k, \Omega_k\}$. The corresponding epochs are $\{\tau_1, \tau_2, \dots, \tau_t\}$. Note that using the method presented herein, one or more orbit elements can be validated simultaneously. Given this time ordered sequence of observation data, the classical exponential smoother computes the smoothed time series (denoted by tilde) according to the following recursion relation:

$$\tilde{\xi}_k = \alpha_t \xi_k + (1 - \alpha_t) \tilde{\xi}_{k-1} \quad (1)$$

where $\alpha_t \in [0, 1]$ is the *smoothing parameter* that controls the degree of smoothing. A high value of α_t will lead to the majority of the weight being placed on the most recent observations, whereas a smaller value of this parameter will imply the observations further in the past will have more influence on the forecast value. Eq.(1) is a recursive computing scheme in which forecasts are updated as each new observation arrives. A one-step-ahead prediction (denoted by overhat) from exponential smoothing is given by the most recent smoothed value:

$$\hat{\xi}_{k+1|k} = \tilde{\xi}_k \quad (2)$$

The classical Holt forecasting model is:

$$\tilde{\xi}_k = \alpha_{1t} \xi_k + (1 - \alpha_{1t}) \tilde{\xi}_{k-1} \quad (3)$$

$$L_k = \alpha_{2t} (\tilde{\xi}_k - \tilde{\xi}_{k-1}) + (1 - \alpha_{2t}) L_k, \quad \alpha_{1t}, \alpha_{2t} \in [0, 1] \quad (4)$$

Eq.(3) is called the level equation whereas Eq.(4) is called the trend equation. One-step-ahead forecast is obtained from:

$$\hat{\xi}_{k+1|k} = \tilde{\xi}_k + L_k \quad (5)$$

The absolute value of the forecast error for both methods is simply:

$$|\epsilon_k| = |\xi_k - \hat{\xi}_k| \quad (6)$$

A notable deficit of the traditional exponential and Holt forecasting models formulated in Eqs.(1)-(4) is that prediction using these models is unduly influenced by observation values that are unusually high or low relative to the to-date sequence members. In the context of orbital element anomaly detection, this would imply that the predicted value of the element immediately following an out-of-family observation would be biased toward that observation, and if the next OD value returns to the “normal” level, then the subsequent several in-family values would be erroneously tagged as unusual. On the other hand, if the few OD values immediately following an actual space event are indeed atypical relative to the majority of the prior-to-event values, then a forecasting model not robust to outliers in the time series may fail to label *all* of the first few post-event values as being out-of-family. To counter these issues, robust versions of exponential and Holt smoothing methods recently proposed by Gelper et al. are used in this work.⁷ Following the modifications proposed by Gelper et al., when a forecast has an absolute one-step-ahead prediction error exceeding a certain threshold, then the corresponding observation is replaced by a “cleaned” one, labeled ξ_k^c , one that results in a forecast error more “typical” of the historical forecast errors. The *robust* versions of the exponential and Holt models are:

$$\text{Robust Exponential: } \tilde{\xi}_k = \alpha_t \xi_k^c + (1 - \alpha_t) \tilde{\xi}_{k-1} \quad (7)$$

$$\text{Robust Holt: } \tilde{\xi}_k = \alpha_{1t} \xi_k^c + (1 - \alpha_{1t}) \tilde{\xi}_{k-1} \quad (8)$$

$$L_k = \alpha_{2t} (\tilde{\xi}_k - \tilde{\xi}_{k-1}) + (1 - \alpha_{2t}) L_k, \quad \alpha_{1t}, \alpha_{2t} \in [0, 1] \quad (9)$$

where

$$\xi_k^c = \psi\left(\frac{\epsilon_k}{\rho_k}, \kappa\right) \rho_k + \hat{\xi}_k \quad (10)$$

and

$$\psi(\nu, \kappa) := \begin{cases} \nu & \text{if } |\nu| < \kappa \\ \kappa \operatorname{sgn}(\nu) & \text{otherwise} \end{cases}, \quad \kappa \in \mathbb{R} \quad (11)$$

is a family of the so-called Huber ψ functions. The quantity ρ_k is the called the *estimated scale of forecast errors*, itself dynamically computed through the recursion relation:

$$\rho_k^2 = [\gamma \theta\left(\frac{\epsilon_k}{\rho_{k-1}}, m_\kappa\right) + (1 - \gamma)] \rho_{k-1}^2, \quad \gamma \in \mathbb{R} \quad (12)$$

and the bi-weight loss function $\theta(\cdot, \cdot)$ is defined as:

$$\theta(\nu, m_\kappa) := \begin{cases} m_\kappa [1 - (1 - (\frac{\nu}{m_\kappa})^2)^3] & \text{if } |\nu| < \kappa \\ m_\kappa & \text{otherwise} \end{cases}, \quad \kappa \in \mathbb{R} \quad (13)$$

Eq. (10) implies that if, at a generic validation epoch, the magnitude of the observed element exceeds its forecast value by $\kappa \rho_k$, a certain proportion of the predicted error scale at that epoch, then that observation should be replaced by a tolerance or boundary value of:

$$\xi_k^b = \xi_k^c = \hat{\xi}_k \pm \kappa \rho_k \quad (14)$$

Refer to Fig. 2 for a schematic representation of the cleaning process. Assuming a Gaussian distribution of one-step-ahead forecast errors, a value of $\kappa = 2$ in Eq.(10) replaces any outlier exceeding a 2σ limit by the boundary value. A value of $\kappa = 2$ leads to $m_\kappa = 2.52$.⁷ The smoothing parameter γ in Eq.(12) is selected to be 0.2.

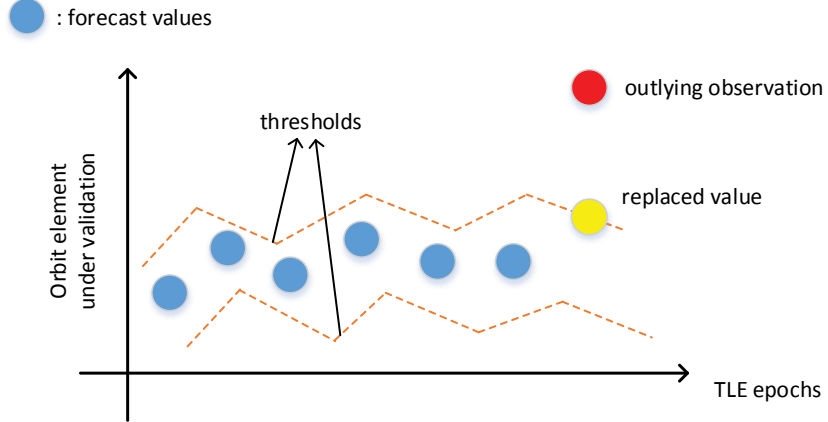


Figure 2: Down-weighting outlying observations

Computational Aspects: There are two main computational considerations that have not been formally addressed yet, namely, the selection of the smoothing parameters α_t , and initializing the recursion relations Eq.(7) - (9) and Eq.(12). As alluded to previously, the smoothing constants determine the sensitivity of the exponential and Holt smoothers to the most recent data points. In this work, the smoothing constants at each OD validation epoch are selected to be those that lead to the best forecasts on the past orbit data. Specifically, the optimal smoothing parameters are those minimize the outlier-robust and data-scale-independent Mean Absolute Scaled (Forecast) Errors (MASE) to date:⁸

$$\alpha_t^* = \arg \min_{\alpha_t \in [0, 1]^n} \frac{t-1}{t} \frac{\sum_{k=1}^t |\xi_k - \hat{\xi}_k(\alpha_t)|}{\sum_{k=2}^t |\xi_k - \xi_{k-1}|}, \quad n = 1, 2 \quad (15)$$

Taking the first p observations of the given time series as the “start-up” series, the following initial condition is used for the exponential smoother:

$$(\tilde{\xi}_{\text{init}})_{\text{exponential}} = \text{Med}\{\xi_1, \xi_2, \dots, \xi_p\} \quad (16)$$

In other words, the initial smoothed observation is the median of the start-up sample or a “typical” value from the sample. Also note that median is used as a measure of typicality instead of mean because of its known robustness to outliers.⁹ The initial values of the level and trend for Holt’s smoothing model are determined by linearly regressing start-up observations $\{\xi_1, \xi_2, \dots, \xi_p\}$ vs. $\{\tau_1, \tau_2, \dots, \tau_p\}$

$$(\tilde{\xi}_{\text{init}})_{\text{Holt}} = mp + c \quad (17)$$

$$L_{\text{init}} = m \quad (18)$$

where m is the slope of the linear regressor through the start-up samples, and c its intercept. Instead of using the outlier-sensitive least squares regression (with a 0% breakdown point) to compute m and c , a Thiel-Sen-Siegel repeated median estimator (with a 50% breakdown point) is utilized

herein:¹⁰

$$m = \text{Med}_{i=1,\dots,p} \text{Med}_{j=1,\dots,p, j \neq i} \frac{\xi_i - \xi_j}{i - j} \quad (19)$$

$$c = \text{Med}_{i=1,\dots,p} (\xi_i - mi) \quad (20)$$

For both the smoother models, the estimated error scale sequence is initialized by taking the Median Absolute Deviation (MAD) of the forecast errors in the start-up period:

$$\rho_{\text{init}} = \text{Med}_{k=1,\dots,p} |\epsilon_k - \text{Med}_{k=1,\dots,p} \epsilon_k| \quad (21)$$

Note that the estimator on the RHS of Eq.(21) uses the sample median twice, first to estimate the center of the error sequence to form the set of absolute residuals about the sample median $|\epsilon_k - \text{Med}_{i=1,\dots,p} \epsilon_i|$, and then to compute the sample median of these absolute residuals. MAD is a more robust estimator of scale than sample standard deviation, as the latter is greatly affected by the presence of outliers. Using MAD, the effect of atypical OD data points even in the start-up period is prevented from influencing future error estimates, thus minimizing the risk of spurious event detections.

Algorithm Description

Although the analysis presented in this paper is applicable to any time-ordered sequence of orbital states, the data for the examples presented in the following section are mined from the TLE catalog published on the world wide web by CelesTrak.¹¹ The algorithm steps for each RSO under validation are enumerated below, and summarized in the flowchart of Fig.3:

- 1) At a generic validation epoch t , retrieve the latest orbit state from a suitable source S_1 (in this case, the TLE database). Parse the state into the Keplerian set $\{a_t, e_t, i_t, \omega_t, \Omega_t\}$.
- 2) For an element $\xi_t \in \{a_t, e_t, i_t, \omega_t, \Omega_t\}$ under validation, query the orbit state data source over a user-selectable look-back interval Δt_{lb} . The default setting for Δt_{lb} is 120 days for LEO satellites with typically more frequent TLE updates and 180 days for GEO satellites with typically less frequent TLE updates. However, if one or more maneuvers is deemed to have occurred in $[\tau_t - \Delta t_{lb}, \tau_t]$ (details in the sequel), then truncate the time series prior to this event before passing the series for statistical processing. Label this time series $\xi = \{\xi_k : k \in \mathbb{I}\}$, $\mathbb{I} = \{1, 2, \dots, t\}$.
- 3) If the time series from step 2 has length less than or equal to p , the start-up length, no conclusion is drawn regarding the statistical typicality of ξ_t relative to its own history, and as such, return its validation label as “Inconclusive” and store this result in the database (S_2). Wait for the next data feed, and on receipt, increment t by 1 and GOTO step 1.
- 4) If the time series length is greater than p , perform smoothing with the “cleaned” observation (see Eq.(10)), compute the absolute prediction error ϵ_t normalized absolute prediction error:

$$\epsilon_{\text{norm},t} = \frac{|\epsilon_t|}{\text{Med}\{\rho_1, \dots, \rho_t\}} \quad (22)$$

for the appropriate smoothing model depending upon orbit element and regime, as alluded to earlier. Note that Eq.(22) measures the current prediction error in terms of typical, to-date error scale. One of the following cases will arise:

- i) The normalized prediction error is less than an “upper threshold for no concern” ($\eta_{u,valid}$), and the time gap $\Delta_t = \tau_t - \tau_{t-1}$ between the current and previous OD epoch does not exceed a specified factor of the median OD gap $\Delta_{t,Med} = \text{Med}\{\tau_{t-1} - \tau_{t-2}, \tau_{t-2} - \tau_{t-3}, \dots, \tau_2 - \tau_1\}$ to date, i.e.

$$\epsilon_{norm,t} < \eta_{u,valid} \wedge \Delta_t < \lambda \Delta_{t,Med}, \lambda \in \mathbb{R}_{>0}$$

In this case, mark the current element ϵ_t as in-family or “Valid”, store the result in S_2 and GOTO step 1. Note that it is necessary to impose a condition on the OD time gap Δ_t because it has been noticed that there sometimes occur erratic delays in TLE publication by USSTRATCOM. Recognizing the fact that the smoother models effectively perform zero (exponential) or first (Holt) order hold extrapolation on smoothed data to predict the next observation, it is easy to see that an out-of-family Δ_t may itself cause an otherwise ordinary ϵ_t to be labeled as anomalous. Therefore, a check must be present to prevent this from happening.

- ii) The normalized prediction error lies between $\eta_{u,valid}$ and a “lower threshold for invalid OD”, $\eta_{l,invalid}$, accompanied by a larger-than-usual gap between the current and the previous observation epochs, i.e.

$$\epsilon_{norm,t} \in [\eta_{u,valid}, \eta_{l,invalid}] \wedge \Delta_t \geq \lambda \Delta_{t,Med}$$

In this case, a higher-than-normal prediction error might have been caused due to a longer-than-usual interval between successive state timestamps, and as such, no conclusion can be drawn regarding the validity of ϵ_t . Therefore, mark the observation ξ_t as “Inconclusive”, store the result in the database S_2 , return to step 1.

- iii) The normalized prediction error $\epsilon_{norm,t} \in [\eta_{u,valid}, \eta_{l,invalid}]$ and current-to-previous OD gap $\Delta_t < \lambda \Delta_{t,Med}$. If this is the case, call the observation “Unexpected”, store the result, and return to step 1.
- iv) $\epsilon_{norm,t} > \eta_{l,invalid}$. In this case, ϵ_t is considered unambiguously out-of-family or “Invalid”, regardless of the OD time gap Δ_t . However, if $\xi_t \in \{a_t, i_t\}$, check if the current element is the l^{th} , $l < p$, successive invalid element in the sequence $\{\xi_{t-l}, \xi_{t-l+1}, \dots, \xi_t\}$
 - a) If yes, then it is possible that the preceding $l-1$ data points represent a post-in-plane/out-of-plane maneuver sequence. Modify, in the database S_2 the validation label of the first element ξ_{t-l} of the sequence from “Invalid” to “Possible Maneuver”, and the labels of $\{\xi_{t-2}, \dots, \xi_t\}$ from “Invalid” to “Inconclusive”, and go back to step 1.
 - b) If not, store the current validation result in S_2 as “Invalid” and return to step 1.

5) Repeat.

The default (and arbitrary) choices for the parameters adopted here based on running a large number test cases from various orbit regimes are: $p = 10$, $\eta_{u,valid} = 4$, $\eta_{l,invalid} = 8$, $\lambda = 8$, $l = 5$. Note that in the above treatment, both “Unexpected” and “Invalid” express statistical atypicality of an element, albeit in an increasing order of severity.

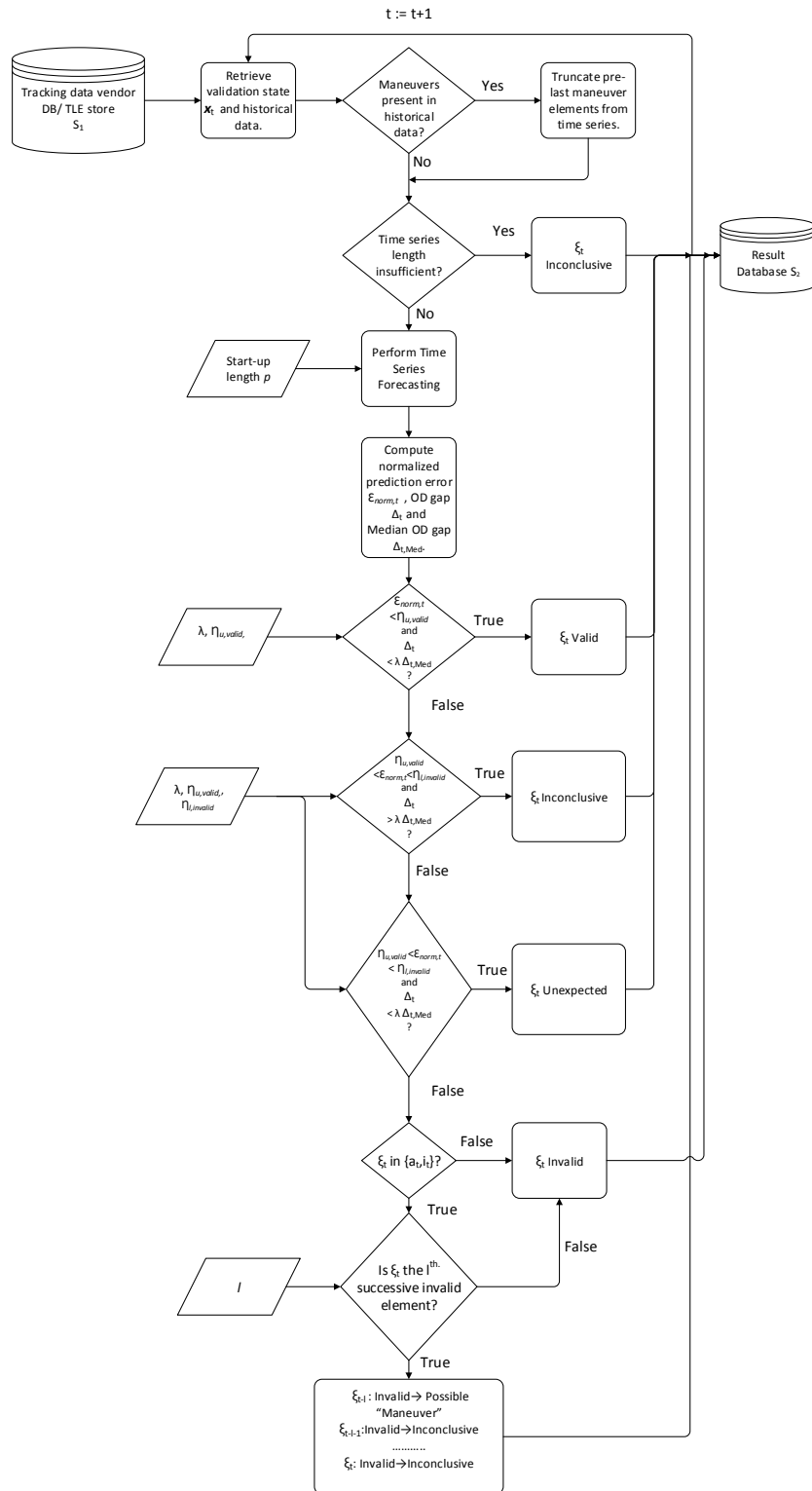


Figure 3: Space event detection algorithm flowchart

APPLICATIONS

The Galaxy-15 Case

Orbital Science Corporation-built and Intelsat-operated Galaxy-15 (SSN # 28884) is a geosynchronous communication satellite that was launched in October 2005 and placed at 133° W longitude, and is mainly used for relaying DirectTV signals within North America. The spacecraft operated normally for more than 4 1/2 years until the occurrence of an anomaly on April 5 2010 at 09:48 UT when the vehicle suddenly ceased responding to station-keeping ground commands. However, it was still able to maintain attitude, and keep its GPS WAAS broadcasting functionality in tact. The upshot of this was that Galaxy-15 began drifting eastward uncontrollably with its operators maintaining precise knowledge its orbital position. It was conjectured that heightened geomagnetic activity associated with a solar storm initiated this malfunctioning of its command control system. Intelsat was reported to have reestablished control of the vehicle on December 23, 2010 when it was located at about 93° W longitude, following which the satellite started responding to commands again. It transpired that the vehicle's reaction wheels eventually saturated, leading to a loss of control authority required for proper sun-ward orientation of the solar panels. This in turn led Galaxy-15's command unit to reboot, making it receptive to ground commands once more.¹² However, Galaxy-15's free drift through the heavily crowded geobelt gave rise to multiple cross-tagging incidents with other RSOs, and these appeared as trajectory inaccuracies in the public TLE catalog.¹³ Equipped with the knowledge that Galaxy-15 did not undergo any maneuver in its drifting journey, the objective of this test case is to ascertain whether some of the cross-tagging events could be identified as outliers by the algorithm under study.

Fig. 4 shows the evolution of the Galaxy 15 semi-major axis starting from October 5, 2009 to December 10, 2011. It is apparent from the graph that the vehicle was indeed holding its altitude more or less constant until control was lost, after which its semi-major axis started decaying, a trend consistent with its reported eastward drift. Marked with asterisks on the figure are data inconsistencies that resulted from Galaxy-15's cross-tagging with other RSOs in the geobelt, notable amongst them being its mis-association with Galaxy-18 during a fly past that occurred around August 13, 2010.¹³ A large change in semi-major axis is also evident in January 2011, which is possibly a maneuver executed after control was regained.

Table 1 enumerates the epochs of the anomalies detected during Galaxy-15's free drift, along with the corresponding normalized prediction error magnitudes. It is interesting to observe that relatively high values of $\epsilon_{\text{norm},t}$ typically accompany cross-tagging incidents. Note that the association of high prediction error values with their cause (such as cross-tagging) with certainty is beyond the scope of this work; the motivation for including the event label with detected anomaly in Table 1 is to emphasize that high prediction errors detected by the algorithm under discussion have indeed been caused by actual space events identified elsewhere.¹³

Table 1: Galaxy-15 Event Detection Results

τ_t	\hat{a}_t , km.	a_t , km.	$\epsilon_{\text{norm},t}$	Event
4/9/10, 7 : 56 : 56.45	42164.12	42166.19	167.51	Beidou, Elektro-L1 cross tag
4/10/10, 2 : 42 : 09.25	42164.26	42164.04	7.90	Unknown
4/10/10, 14 : 25 : 28.60	42164.09	42163.98	7.27	Unknown
4/11/10, 6 : 07 : 01.55	42164.00	42163.93	5.49	Unknown
4/13/10, 13 : 47 : 26.74	42163.61	42163.85	22.44	Unknown
4/14/10, 15 : 16 : 08.08	42163.59	42163.82	19.40	Unknown
4/15/10, 2 : 49 : 27.79	42163.94	42163.62	39.94	Unknown
4/26/10, 13 : 51 : 21.39	42162.87	42162.69	12.39	Unknown
5/4/10, 14 : 52 : 01.60	42162.22	42161.83	15.82	Unknown
5/7/10, 12 : 16 : 22.30	42161.96	42161.50	17.37	Unknown
5/11/10, 12 : 48 : 51.93	42161.58	42161.04	17.00	Unknown
5/12/10, 22 : 17 : 44.96	42160.51	42161.92	38.89	Elektro-L1, Arabsat, SkyTerra-1 cross tag
5/13/10, 14 : 59 : 46.23	42160.61	42160.86	7.18	Unknown
5/19/10, 13 : 18 : 00.02	42160.31	42160.97	17.93	Arabsat 5B cross tag
5/24/10, 12 : 59 : 39.28	42160.41	42160.12	7.54	Unknown
5/28/10, 13 : 07 : 00.35	42159.46	42158.53	21.76	SES-1 cross tag
6/1/10, 21 : 36 : 00.00	42158.78	42159.05	5.75	Unknown
6/2/10, 20 : 48 : 02.53	42158.84	42159.84	21.44	AMC 11 cross tag
6/4/10, 13 : 28 : 48.097	42158.88	42158.56	6.68	Unknown
06/29/10, 9 : 11 : 08.77	42157.23	42156.62	7.33	Unknown
06/30/10, 13 : 06 : 30.41	42157.10	42156.40	7.89	Ciel 2 cross tag
7/7/10, 18 : 27 : 55.43	42156.10	42156.75	6.53	Unknown
7/21/10, 17 : 33 : 42.061	42155.18	42155.73	5.66	Themis-A, Hylas-1 cross tag
8/12/10, 8 : 34 : 48.46	42153.54	42154.53	15.62	Galaxy-18 cross tag
8/13/10, 16 : 01 : 05.71	42153.75	42150.68	49.69	Galaxy-18 cross tag
1/1/11, 12 : 01 : 29.01	42150.58	42138.38	267.62	Possible in-plane maneuver

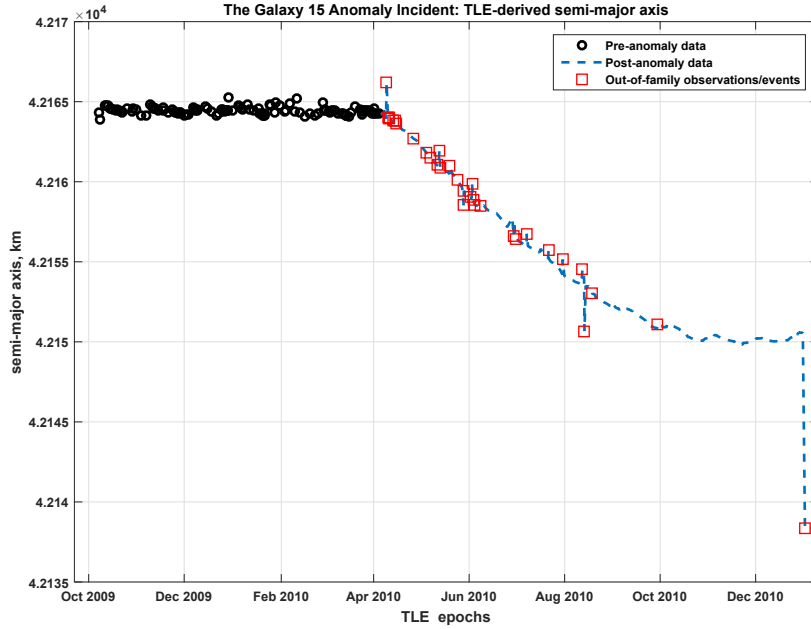


Figure 4: The Galaxy-15 Incident

Orbview-3 Deorbit

GeoEye Orbview-3 (SSN # 27838), launched in June 2003, was a polar orbiting commercial remote sensing satellite that completed its nominal mission in March 2007. The satellite's attitude control system was reported to be fully functional at that point. Although the vehicle's orbit would have naturally decayed, resulting in its eventual reentry into Earth's atmosphere within the recommended 25 year period, GeoEye decided to execute a controlled de-orbit and reentry so as to minimize the risk of conjunction with other LEO objects, especially the International Space Station (ISS). The de-orbit was implemented in two phases: Phase 1 consisted of 6 orbit-lowering maneuvers that lowered the apogee below that of the ISS, whereas Phase 2 included 4 additional maneuvers to further decay the perigee and effect a reentry and over the Pacific Ocean.¹⁴

The actual epochs (or ignition times) of the maneuvers as executed and maneuver goals taken from reference 14 are tabulated in table 2. Out of the six Phase 1 maneuvers, the first one was a short duration (30 sec.) test/calibration burn, the second one was an unplanned debris collision avoidance burn, also of short duration, whereas the rest were planned, longer duration orbit lowering burns each lasting 280+ seconds.

Fig. 5 shows the altitude of the satellite starting from December 1, 2010, 12:22:07.17 UTC up to March 13, 04:42:18..09 UTC, the latter date being the epoch of the last available TLE for this object from Celestrak. The abrupt changes in the satellite altitude, arising out of orbit-lowering ΔV 's is clearly discernible from the figure. The altitudes at the maneuver epochs as detected by the method under study are marked with square markers. Table 3 summarizes the event detection results for this case. Note that while all six of the Phase 1 maneuvers were identified, only two of the four Phase 2 maneuvers were detected. To investigate the reason, it may be recalled from the algorithm description that an already-detected anomaly is not immediately classified as a maneuver,

but rather, it is recognized as a possible maneuver only if l successive values counting the anomaly in question are consistently marked as “Invalid”. If at least l data points are not available past an anomalous OD, then a maneuver will not be captured. In the present case, the detection of the last two maneuvers fails precisely owing to this lack of data. Also note the slight difference in time between the ignition times reported in table 2 and the maneuver epochs appearing in table 3. This lag is attributed to new TLE generation process after the occurrence of an event.

Figure 6 plots the inclination time-series of the satellite. Abrupt changes are apparent from the graph, with those identified by the event detection algorithm marked with asterisks. From visual inspection, it can be seen that there are no level changes followed by new trends, thus minimizing the likelihood of out-of-plane maneuvers. Indeed, the event detection algorithm has not reported any maneuvers by analyzing the inclination time series; from table 4 it is seen that only “instantaneous” unexpected/invalid ODs are noted, some of them at approximately the same times as the maneuvers were suggested. Collating the information from tables 3 and 4, it is thus a reasonable conjecture that all of the de-orbit maneuvers were planned to be exclusively in-plane, with some transverse thrust component perhaps arising from the non-ideal nature of the thrusting process.

Table 2: Orbview-3 Actual Deorbit Maneuvers

Maneuver No./ Phase	Maneuver Start Time	Maneuver Goal
1/1	12/22/2010, 12:52:34.200	Lower perigee
2/1	1/2/2011, 6:50:32.887	Lower perigee
3/1	1/5/2011, 12:27:50.361	Lower perigee
4/1	1/7/2011, 13:05:49.722	Lower apogee
5/1	1/9/2011, 14:15:51.466	Lower apogee
6/1	1/11/2011, 17:18:25.000	Lower apogee
1/2	3/5/2011, 15:28:03.000	Lower perigee
2/2	3/10/2011, 00:17:36.020	Lower perigee
3/2	3/13/2011, 02:21:37.000	Lower perigee
4/2	3/13/2011, 05:15:50.000	Lower perigee

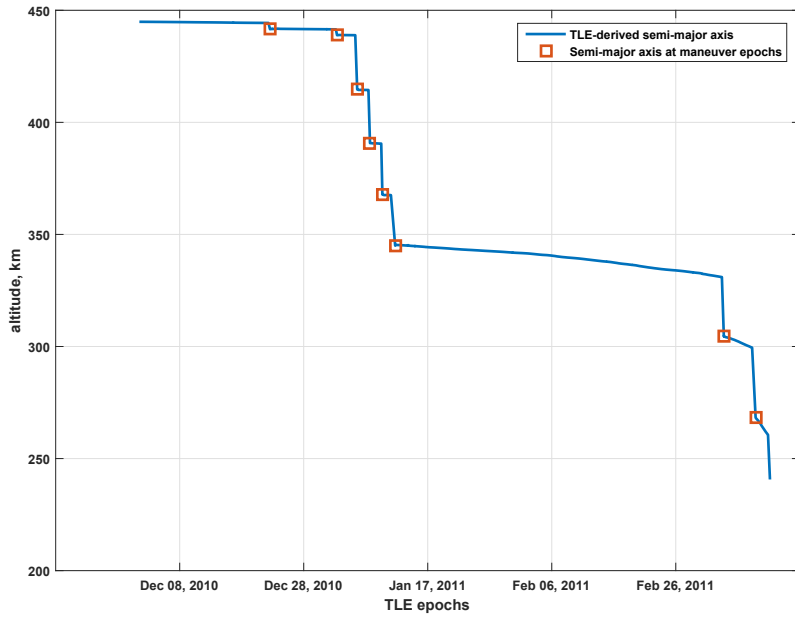


Figure 5: Orbview-3 In-plane maneuvers

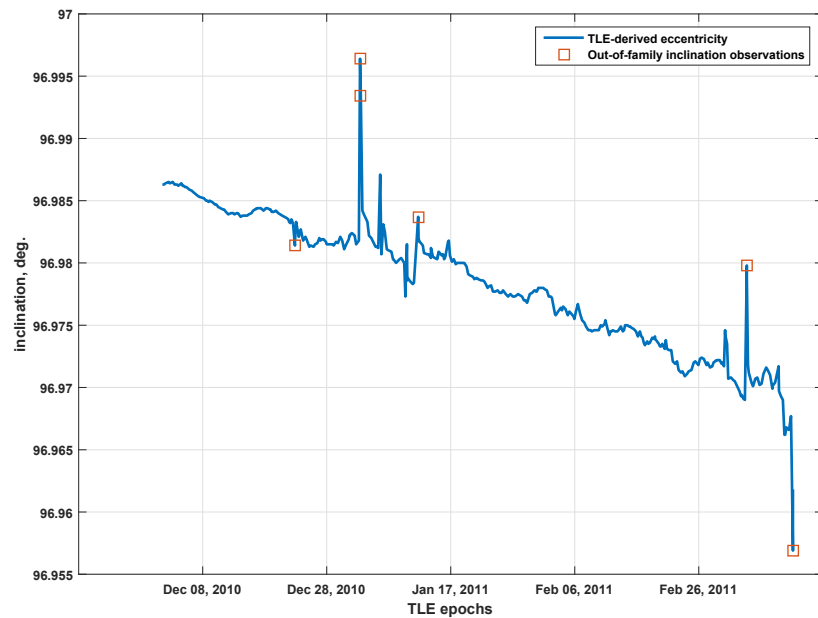


Figure 6: Orbview-3 Inclination Events

Table 3: Orbview-3 Detected In-plane Maneuvers

Event Epoch	$\epsilon_{\text{norm},t}$
12/22/2010, 13:15:22.405	132.42
1/2/2011, 9:14:46.237	98.70
1/5/2011, 15:02:09.0557	1268.55
1/7/2011, 16:25:16.41	6126.18
1/9/2011, 16:02:58.97	959.52
1/11/2011, 18:27:14.31	1773.75
3/5/2011, 18:18:46.83	118.01
3/10/2011, 18:18:46.82	46.59

Table 4: Orbview-3: Results From the Inclination Time Series

Event Epoch	$\epsilon_{\text{norm},t}$	Event
12/22/2010, 21:02:00.00	7.93	Unexpected OD
1/2/2011, 9:14:46.237	29.37	Invalid OD
1/2/2011, 12:30:12.46	22.16	Invalid OD
1/11/2011, 18:27:14.31	6.71	Unexpected OD
3/5/2011, 18:18:46.83	12.07	Invalid OD
3/13/2011, 4:42:18.09	10.57	Invalid OD

THEOS Orbit Control Maneuvers

THEOS (SSN # 33396), Thailand's first Earth observation satellite, was launched on October 1, 2008 and placed in a near-circular Sun-synchronous orbit of nominal altitude 822 km. and nominal inclination 98.7° . Over the period February 2010 to December 2010, the spacecraft underwent three Orbit Control Maneuvers (OCMs), the first two being station-keeping maneuvers and the last one an emergency collision avoidance maneuver to avoid a piece of debris.¹⁵ The first OCM, split in two sub-maneuvers and intended to be purely in-plane, reportedly took place on February 10, 2010. This was a Ground Track Maintenance maneuver targeted to achieve a semi-major axis decrease of 40 km. which in turn was meant to check the vehicle's orbital perturbation-induced ground track drift and bring it back into the mission-required control band. The second OCM, executed on November 23, 2010, was intended to be a pure *inclination change* maneuver aimed at correcting the ascending node local time (Local Solar Time, LST) of the THEOS orbit.¹⁵ The target LST of THEOS is 22:00 hours within a ± 2 mins. tolerance band. However it is known that for low-altitude Sun-synchronous orbits, drag and lunisolar perturbations gradually disrupt Sun-synchronism, effectively altering the LST in the process. The out-of-plane maneuver of November 23, 2010 was designed to impart an inclination change of 0.0895° in order to revert the LST into its desired tolerance band. This change in inclination was achieved in practice by distributing a single ΔV into four sub-maneuvers at the orbit descending nodes. The third and final maneuver of the year took place on December 15, 2010, performed in order to avoid conjunction with an unknown object. This was again an in-plane maneuver designed to lower the spacecraft orbit by 80 km., and was initiated based on a JSpOC (Joint Space Operations Center) Conjunction Analysis Report.¹⁵ Table 5 summarizes the maneuvers as reported in reference 15.

Figures 7 and 8 plot the semi-major axis and inclination evolution from January 1, 2010 to December 31, 2010. Also marked on the figures are the maneuvers suggested *based on the publicly available TLE data*. Attention is drawn to the fact that the event detection algorithm has recognized *three* instances of *tangential thrusting* instead of the intended two, and a *single* instance of *normal thrusting*, see tables 6 and 7. Indeed, it is reported in reference 15 that although OCM 2 was planned to be a pure inclination change maneuver, in practice, parasitic tangential thrust resulted in an unexpected change in the semi-major axis by 166 km., which was captured by the algorithm under study. It may further be noted that the detected event epochs lag the reported burn centroid times, and that instead of detecting the sub-maneuvers, a single cumulative maneuver has been identified in each case. This should not come as a surprise because in addition to the known fact that published TLEs epochs lag actual events, it is also the case that there is necessarily no one-to-one correspondence between actual events TLE updates. It is thus likely that the effect of four consecutive thrusts in quick succession (of the order of the LEO orbital period) was not manifested in a "lumped" fashion in the published TLEs until later.

Table 5: THEOS Reported Maneuvers

Maneuver Number	Burn Centroid Time	Maneuver Intended Effect
OCM 1, Burn 1	2/10/2010, 19:49:40	Raise orbit
OCM 1, Burn 2	2/10/2010, 21:31:08	Lower orbit
OCM 2, Burn 1	11/23/2010, 19:49:40	Change inclination
OCM 2, Burn 2	11/23/2010, 21:31:08	Change inclination
OCM 2, Burn 3	11/23/2010, 23:12:35	Change inclination
OCM 2, Burn 4	12/15/2010, 00:54:03	Change inclination
OCM 3	3/5/2011, 03:34:53	Lower orbit

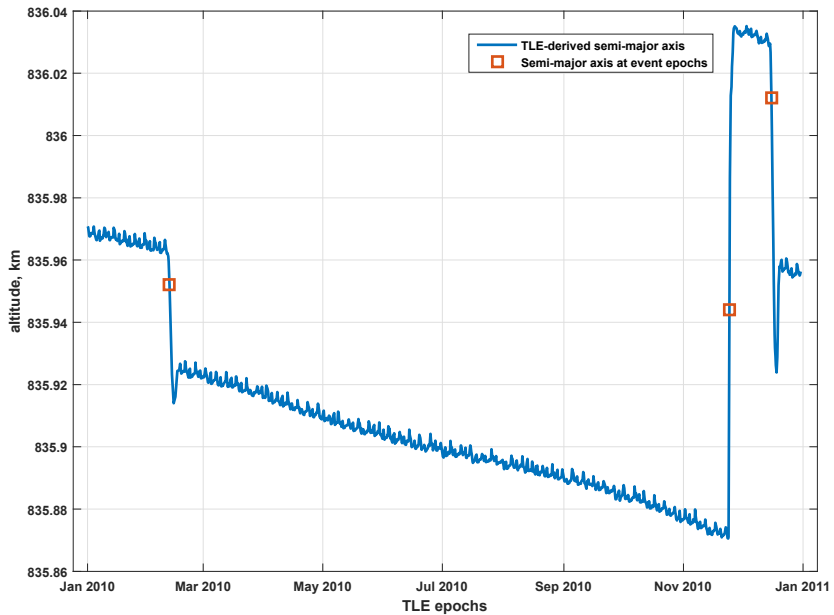


Figure 7: THEOS In-plane Maneuvers

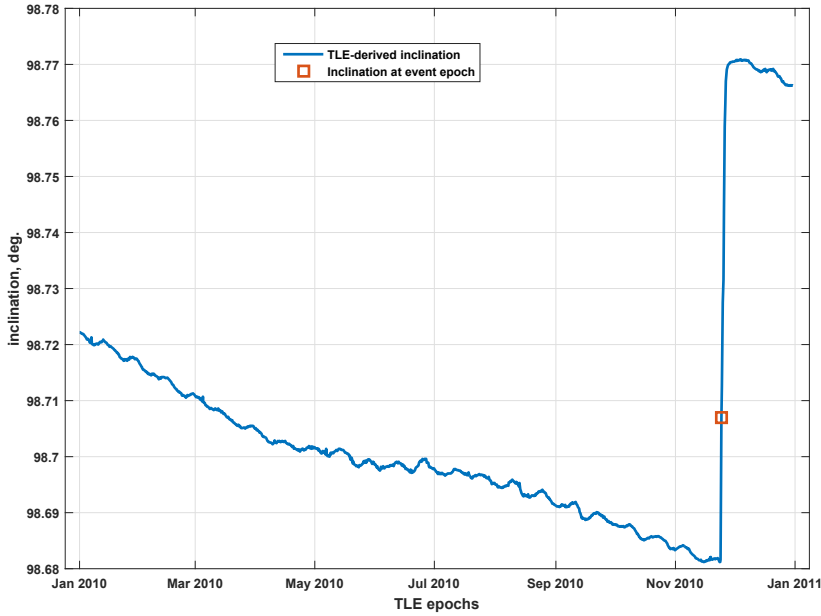


Figure 8: THEOS Out-of-plane Maneuver

Table 6: THEOS Detected In-plane Maneuvers

Event Epoch	$\epsilon_{\text{norm},t}$
2/11/2010, 19:22:00.70	9.98
11/24/2010, 11:00:46.99	93.00
12/15/2010, 20:53:58.04	16.29

Table 7: THEOS Detected Out-of-plane Maneuver

Event Epoch	$\epsilon_{\text{norm},t}$
11/24/2010, 11:00:46.99	164.56

CONCLUSIONS

This paper presented a novel method for flagging newly-detected orbit states as in/out-of-family using outlier-robust time series forecasting techniques. A unique feature of this algorithm is that, unlike some of the existing event detection methods in the open literature, it is not restricted to a particular orbit regime, such as the LEO or GEO. Apart from being able to detect anomaly in each component of an orbit state, the algorithm is also able to identify events as “maneuvers” if abrupt and permanent change in the orbit’s shape and orientation occurs. Furthermore, its usefulness is not restricted to detecting maneuvers only; maneuvers were indeed identified, and further classified as in/out-of-plane, but so were other instances of anomalous OD as borne out by its sensitivity to

anomalies arising from orbit mis-associations. It is also worthwhile to note that validation of an orbit state is based on time-series prediction using explicit algebraic expressions, requiring minimal computational effort, thus making the software implementation a suitable component of an on-line space event monitoring system for an increasingly populous space catalog.

One of the assumptions implicit in the time series forecasting methods adopted in this paper is that the series of observations or OD epochs under consideration is evenly-spaced. This is approximately true for regularly tracked objects in the space catalog. Another factor worth noting is the fact that for suggesting maneuvers with some degree of confidence, several post-event observations are necessary in order to be able to discern a trend in the level-shifted post-event series. In the absence of this requisite number of observations, a maneuver-type event may not be detected as such, although an anomaly will be noted. An instance of this behavior was seen in the Orbview-3 example.

ACKNOWLEDGMENTS

The author wishes to thank Dr. Vince Coppola of Analytical Graphics Inc. for his insights during the many helpful discussions during this work. Many thanks also to Dr. Dan Oltrogge of Analytical Graphics Inc. for sharing the epochs and satellite names for the cross-tagging instances in the Galaxy-15 example.

REFERENCES

- [1] W. Rathgeber, “Europe’s Way to Space Situational Awareness (SSA),” tech. rep., European Space Policy Institute (ESPI) Report, No. 10, 2008.
- [2] Russell Patera, “Space Event Detection Method,” *AIAA/AAS Astrodynamics Specialist Conference and Exhibit*, Keystone, Colorado, 2006.
- [3] Raymond L. Swartz, Jr., John Coggi and Justin McNeill, “A Swift SIFT for Satellite Event Detection,” *AIAA/AAS Astrodynamics Specialist Conference*, Toronto, Ontario Canada, 2010.
- [4] Tom Kelecy, Doyle Hall , Kris Hamada and Maj. Dennis Stocker, “Satellite Maneuver Detection Using Two-line Element (TLE) Data,” *AMOS Technical Conference Proceedings*, Wailea, HI, 2007.
- [5] Stijn Lemmens and Holger Krag, “Two-Line-Elements-Based Maneuver Detection Methods for Satellites in Low Earth Orbit,” *Journal of Guidance, Control, and Dynamics*, Vol. 37, No. 3, 2014, pp. 860–868.
- [6] Everette S. Gardner, Jr., “Exponential Smoothing: The State of the Art,” *Journal of Forecasting*, Vol. 4, No. 1, 1985, pp. 1–28.
- [7] Sarah Gelper, Roland Fried, and Christophe Croux, “Robust Forecasting with Exponential and Holt-Winters Smoothing,” *Journal of Forecasting*, Vol. 29, No. 3, 2010, pp. 285–300.
- [8] Rob J. Hyndman and Anne B. Koehler, “Another Look at Measures of Forecast Accuracy,” *International Journal of Forecasting*, Vol. 22, No. 4, 2006, pp. 679–688.
- [9] Ricardo A. Maronna, Douglas R. Martin, and Victor J. Yohai, *Robust Statistics: Theory and Methods*. Wiley, 1st ed., 2006.
- [10] Peter J. Rousseeuw, “Least Median of Squares Regression,” *Journal of the American Statistical Association*, Vol. 79, No. 388, 1984, pp. 871–880.
- [11] “Current Space Track NORAD Two-Line Element Sets,” <http://www.celestrak.com/SpaceTrack/>. Accessed: 01/19/2016.
- [12] Doyle Hall, “AMOS Galaxy 15 Satellite Observations and Analysis,” *AMOS Technical Conference Proceedings*, Wailea, HI, 2011.
- [13] Daniel L. Oltrogge and Sal Alfano, “Determination of Orbit Cross-Tag Events and Maneuvers with Orbit Detective,” *AAS/AIAA Astrodynamics Specialist Conference*, Girdwood, AK, 2011.
- [14] Timothy Craychee and Shannon Sturtevant, “Mitigating Potential Orbit Debris: The Deorbit of a Commercial Spacecraft,” *AAS/AIAA Astrodynamics Specialist Conference*, Girdwood, AK, 2011.
- [15] P. Navakitanok, A.H. Gicquel, A. Pimnoo, and S. Jaturut, “THEOS Orbit Maintenance: Assessment of 2 Years of Operations,” *Proceedings of the 22 nd. International Symposium on Space Flight Dynamics*, Brazil, 2011.